Portable State of Power Determination of Li-ion Battery Cells

Hidde de Vries
Power Electronics and EMC
University of Twente
Enschede, the Netherlands
vriesdehidde@gmail.com

Maarten Appelman
Power Electronics and EMC
University of Twente
Enschede, the Netherlands
m.b.appelman@utwente.nl

***Abstract*—A novel portable measurement setup, which allows the determination of the state of power (SOP) for li-ion batteries, is introduced through the development of a prototype. The measurement setup performs a hybrid pulsed power characterisation test using a DC-DC converter and a small energy storage system, compared to the currently existing grid-based solutions. The portability allows for a greater range of use cases, for example energy access, at the cost of measurement precision.**

To prove the theoretical concept, a prototype was developed and produced for a single battery cell. The setup was tested and verified by creating a battery model, achieved through data fitting on measurements performed. While there is some inaccuracy in both the measurements and data processing, the generated model shows agreement with measured verification data. The battery SOP is determined from the model, for two different use cases. Overall, it is a promising start to creating a portable SOP measurement system for a full battery pack.

I. Introduction

The advance of photovoltaic energy generation has reduced the worldwide dependence on fossil fuels [1]. It has also increased global access to energy, as solar panels can be installed anywhere and do not require the infrastructure an electrical grid requires [2]–[4]. Energy access is important, as it can improve the quality of life through, for example, clean cooking or consistent light in the evening [5], [6].

Excess energy generated by the solar panels can be stored in battery cells, which is already done for some microgrids [7]. However, fossil fuel generators are often still used as backup [3], as it is hard to determine how much usable energy is stored in the battery pack. This energy is dependent on the type of battery used, the state of charge (SOC) and the age of the battery, as battery cell capacity degrades due to lifetime age and charging cycles. Furthermore, the amount of power pulled from the battery is important to know, because the current and voltage limits of the battery can be reached before it is empty.

This paper focuses on determining the maximum power that can be drawn from a battery cell without reaching voltage or current limits, depending on the total time the power is drawn and the initial battery charge. This is also known as the state of power (SOP) of the battery.

The SOP will be determined using a battery model, which is created from measurements using hybrid pulsed power characterisation (HPPC) tests. A short ($\sim 30\,\mathrm{s}$) current pulse is applied to the battery, and later pulled from it. The battery model is determined based on the voltage response to this current.

The prototype developed is designed for improving energy access, which adds some extra requirements to the system. Specifically, the measurements will be performed at remote locations without a guaranteed reliable source of energy. Most off-the-shelf battery measurement systems require a stable grid connection and are hard to move around. To solve these issues, a portable solution is introduced in this paper, which uses its own small energy storage to perform the tests required to determine the SOP.

Several aspects are specifically investigated using a developed prototype. The main question is whether a simple setup is enough to provide all the required measurement data, and whether the unfiltered noise due to the simplicity disrupts the SOP determination. Another focal point is the energy storage system used in the prototype and if it interferes with the measurements.

Although the prototype developed is not perfect, all aspects show promising results and only minor changes are required to make it work well.

Before the prototype itself is shown, the theory behind the SOP determination is first discussed in Section II, which includes the specific battery model and how the parameters of the model are gathered. This is done in two ways, using the HPPC test for the prototype itself and using electrochemical impedance spectroscopy (EIS) for model verification. With the relevant theory known, the measurement setup itself is discussed in Section III. This measurement setup is the main part of the developed prototype, and is focused on as it is relevant for the data gathering. The results are shown in Section IV, starting with the measurement verification.The HPPC test results are shown next, and compared to the results gathered from the EIS test. At the end of the results, the model verification and the SOP itself are displayed. The results gathered are discussed in Section V. This includes how the design and data processing can be improved, and some changes to go from the prototype to a usable product. The paper is concluded after this discussion, in Section VI.

II. Theory

For the theory, the battery model used will be discussed first. A battery model is the main, but not only method used to determine the SOP. Another option is using a large data set of battery measurements and extrapolating the required data using machine learning. In comparison, generating the battery model takes little data, which is why it is used.

After the battery model is shown, the method in which the model parameters are found is discussed. This starts with a short comparison between the HPPC and EIS tests and then expands on the HPPC test and how it is used.

The HPPC model generated is not fully validated with the EIS test, as low-frequency voltage responses are hard to gather precisely. Therefore, the model is also validated through a longer measurement of the battery, which is compared to the generated battery model.

A. Battery model

The model would ideally represent the behaviour of the battery as closely as possible, in all conditions. This requires representing all chemical processes occurring in the battery, which requires a significant amount of data processing and a lot of initial data to generate the model [8]. To reduce the calculations and data gathering, a simpler model is used which represents some of these chemical processes as electrical components. This results in a less precise model, but it is considered a good balance between accuracy and complexity [9]–[12]. This model can be seen in Figure 1.

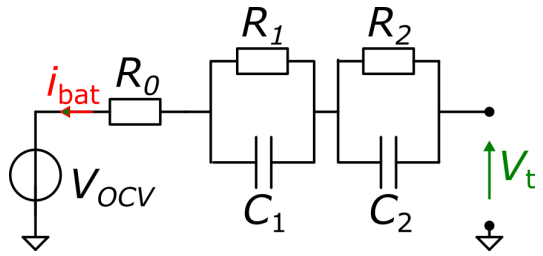

Fig. 1: 2^{nd} order equivalent circuit battery model

In the model, the voltage source V_{OCV} depicts the open circuit voltage (OCV) of the battery. V_t is the terminal voltage, which is measured at the terminals of the battery. R_0 represents the instantaneous resistance in the battery, for example the resistance of the internal plates. The other resistors and capacitor pairs represent chemical processes with a limited reaction speed. The second-order model only depicts the two processes with the most pronounced voltage response. While the exact processes are dependent on the battery used, for most li-ion batteries the two main ones are a fast voltage response due to the chemical reaction at the surface of the electrodes, and a slower response due to the diffusion of ions in the electrolyte of the battery [13].

The SOC of the battery is not depicted in this model. Instead, the parameters of the depicted model change according to the SOC. Because of this, for the final model, the measurements will need to be performed for a range of SOCs.

B. Model parameter determination methods

Two main methods are commonly used to determine the parameters of the model, the HPPC and EIS methods. The HPPC method is used for the measurement setup itself, while part of the battery model verification is done using the EIS method.

The HPPC method works by pushing a square wave current, with an amplitude in the order of 1C and a length of about 10 seconds, into the battery. After a short rest time of 30 seconds, the same current pulse is pulled from the battery [14]. The battery model is determined using the voltage response to these pulses. The specific data processing required is discussed in Section II-C.

The EIS method uses the frequency domain for the measurements. A small voltage oscillation is created on the battery by controlling the current, from which the impedance of the battery is found. By performing a frequency sweep of this oscillation, the impedance at different frequencies is found and can be used to generate a battery model [12].
When comparing the two methods, the EIS method uses a $10\,\mathrm{mV}$ amplitude sine wave, which requires precise voltage and current measurements. The HPPC test uses a higher current than the EIS test, which in turn produces a larger change in voltage at the battery terminal [10]. The HPPC test is therefore less affected by measurement errors. Furthermore, the EIS test requires more time to perform the test due to the frequency sweep. It has been shown that the model parameters are close when comparing both methods, within a 5% relative error for a first-order model [15]. Because of this, part of the verification of the HPPC method is done using the EIS measurements. However, the very low-frequency measurements were imprecise, which is why only part of the model is verified.

Due to the larger voltage response of the HPPC test, and therefore lower requirement on the voltage measurement, it is chosen as the method for the portable battery tester. However, it does require more energy due to the higher current used.

To keep the data processing simple for the HPPC test, the current should be as close to a square wave as possible. A short rise and fall time is required to determine the resistance R_0 of the battery model. Specifically, they should be lower than the measurement interval. Additionally, a stable current is required to determine the time-dependent variables of the capacitor-resistor pairs.

The length of the pulse is important for the accuracy of the model, with a longer time resulting in more measurement data which can be processed for a more precise model. This accuracy shows diminishing returns, with a good result after a pulse of 10 seconds, and 30 seconds rest in between pulses for an ideal measurement setup [14]. However, due to noise in the measurements of the developed prototype, this pulse is lengthened to 30 seconds.

The current amplitude should be high to force a large

voltage response, which is less susceptible to measurement noise. The maximum current of the battery used, the high energy density Sanyo NCR18650GA, is 10 A. To prevent the SOC from changing more than 1% during the test, the current amplitude was initially set at 4 A. However, the combination of the longer test time and high current required a larger energy storage system than the initial design, which is why the current was lowered to 1 A. Other combinations with current amplitude and pulse length were tested, but did not improve the results and were therefore discarded.

C. HPPC data processing

Data fitting is used to determine the model parameters from the measured battery voltage. The battery model, shown earlier in Figure 1, is converted to an equation relating the battery voltage to the current, see Equation 1.

$$v(t) = V_{OCV} + R_0 \cdot i(t) + R_1 \cdot i(t) \cdot (1 - e^{-t/(R_1 \cdot C_1)}) \ldots + R_2 \cdot i(t) \cdot (1 - e^{-t/(R_2 \cdot C_2)}) \quad [\mathrm{V}] \quad (1)$$

In this equation, $v(t)$ is the terminal voltage over time, $i(t)$ is the current over time, while V_{OCV}, R_0, R_1, C_1, R_2 and C_2 are the model parameters.

The measurements performed provide $v(t)$ and $i(t)$. The open circuit voltage V_{OCV} is the battery voltage before the current pulses are applied. The other five variables are determined through parameter fitting. This is done in MATLAB for this prototype, using the *fminsearch()* function.

D. Model verification

The battery model generated needs to be verified. While this is partially done by the EIS measurement, R_2 and C_2 are not verified as discussed later in Section IV-C. The full model verification is performed by applying a predetermined set of current pulses to the battery using a battery tester, the Neware BTS-4008. The total charge of these pulses is 0 Ah to prevent any change in the SOC, and therefore in the model parameters. The applied current can be seen in Figure 2.

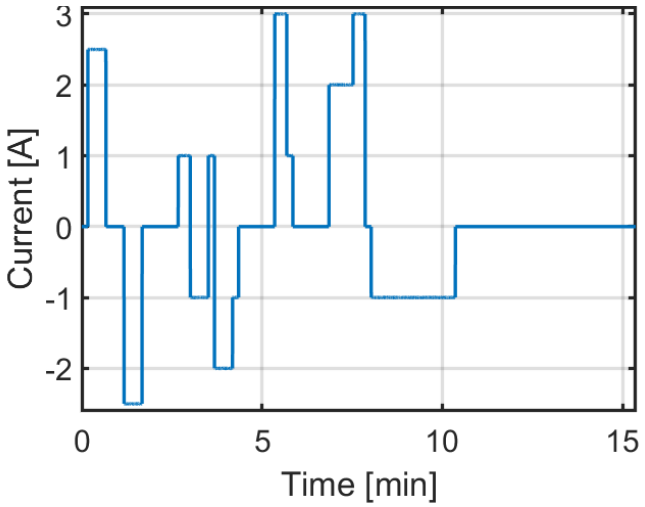

Fig. 2: Current used to verify the battery model

The measured battery voltage while applying this current is shown later in the results, specifically Section IV-D. The verification itself is done by simulating the generated battery model with the same input current, and comparing the measured and simulated voltage.

III. Measurement Setup

The measurement setup is a big part of the physical part of the prototype, combining the DC-DC converter, energy storage and measurements. An overview of the setup can be seen in Figure 3, including the relevant measurements and the fuses to protect the circuit. The measurements and DC-DC converter control are performed with the same microcontroller, the ESP32.

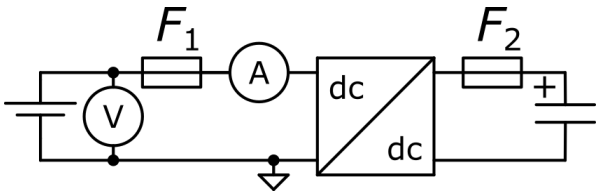

Fig. 3: Simplified overview of the measurement setup, with the battery on the left and a supercapacitor on the right

The relevant choices for the measurements, the energy storage and the DC-DC controller are discussed below.

A. Current measurement

The ACS711KLCTR-25AB-T hall effect current sensor was chosen due to its availability and simple implementation, as it requires only three physical components compared to the 6+ needed for a shunt resistor measurement. It can measure both positive and negative currents, which are converted to a voltage at the output of the sensor chip. This voltage is read in the same way as the other voltages on the PCB.

B. Voltage measurement

The voltage measurements are performed using the two internal ADCs of the microcontroller. The battery voltage and current measurements are placed on separate ADCs. This mitigates any internal delay due to multiplexing, as each ADC can read the voltage of multiple GPIO pins. The voltage measurements all use 100 nF capacitors on the microcontroller input to filter out high-frequency noise.

The measurements are performed once every program cycle of the ESP32, which means the interval between measurements is 10 ms.

C. Energy storage

The energy storage is made with supercapacitors. They need to hold at least 420 J of usable energy for the HPPC test. Due to the DC-DC converter used, the energy storage voltage needs to stay higher than the battery voltage, which limits the usable energy. Because of this, four 50 F supercapacitors, with a maximum voltage of 2.7 V each, are used in series. Because they are in series, a passive balancing circuit is also implemented.

D. DC-DC converter

The DC-DC converter made is bidirectional, to allow for both charging and discharging of the battery. The circuit can be seen in Figure 4. The inductor required for the converter is placed on the battery side, to act as a filter for the battery current. This does require the voltage at the supercapacitor, on the right of the circuit, to be higher than the battery voltage during a battery charging pulse.

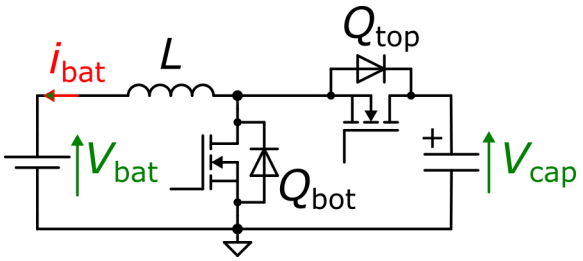

Fig. 4: Bidirectional converter design used in the circuit. Also showing the direction of the battery current used in the results

The two MOSFETs Qtop and Qbot work in complementary mode, and are both driven by PWM signals generated in the ESP32. A $156.25\,\mathrm{kHz}$ signal is used, which allows for a resolution of 9 bits in the duty cycle.

The DC-DC converter should have a short current rise and fall time, with a small current ripple. This allows for easier data processing, as discussed in Section II-B. The short rise time limits the maximum inductance of the inductor, but a higher inductance results in a smaller current ripple. By limiting the rise time to a single measurement interval of the ADC, $10\,\mathrm{ms}$, and a minimum battery voltage of $2.5\,\mathrm{V}$, the following maximum inductance is found:

$$i_L = \frac{1}{L}\int_0^{t_{max}} v_L dt \qquad \text{[A]} \quad (2)$$

$$L = \frac{t_{max} \cdot v_L}{i_L} = \frac{0.01 \cdot 2.5}{10} = 0.0025 \qquad \text{[H]} \quad (3)$$

The theoretical maximum inductance is $2.5\,\mathrm{mH}$. The inductor used is only $220\,\mu\mathrm{H}$, to compensate for any parasitic values of the circuit.

The control for the DC-DC converter is done using a PI controller. The ESP32 controls the duty cycle of the PWM signal based on this controller, with as input the measured battery current. The controller is required because both the battery and supercapacitor voltages change during the current pulse, so the duty cycle has to change continuously. A PID controller was initially planned but never tuned, as the PI controller reached the required current rise time without notable overshoot.

The PI controller also adjusts the duty cycle for a charging or discharging current, as a high duty cycle at the bottom MOSFET will discharge the battery and a low duty cycle will charge the battery.

E. Measurement verification

The measurement setup has to be verified, before the verification of the battery model. This guarantees the model verification detects errors in only the model itself, not errors in the measurements. The measurement verification includes both the current and voltage measurements. For both, the absolute value has to be confirmed, and any drift has to be found. The drift is determined by measuring the voltage at several points in the circuit using an external, high-frequency oscilloscope, the Agilent Infiniium 54854A DSO, while the absolute values are verified with a Fluke 115 digital multimeter.

IV. Results

The results are split into several sections. The measurement setup results are discussed first, with their verification. After this, the HPPC and EIS results are shown, and the comparison between the two. Finally, the battery model is shown and the SOP results are gathered from this model.

All measurements are performed on the developed prototype, a picture of which can be seen in Figure 5, including the relevant sections of the PCB.

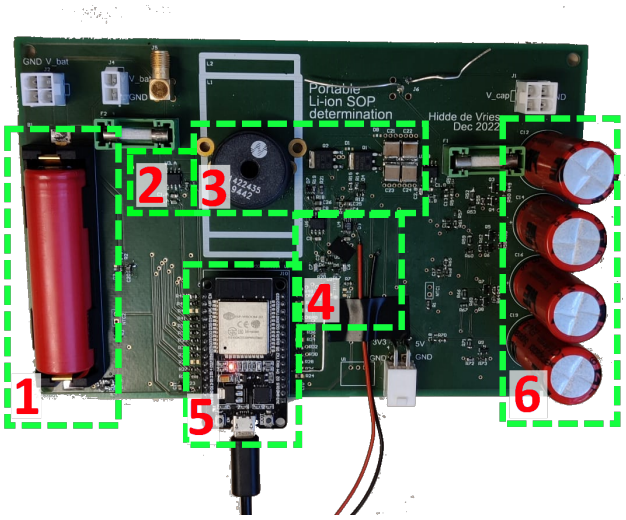

Fig. 5: Overview of the designed PCB, with the different relevant sections of the PCB being: 1) Battery. 2) Battery current sensor. 3) DCDC converter power stage. 4) DCDC converter gate drivers. 5) Microcontroller. 6) Super capacitors.

The measured battery is a Sanyo NCR18650GA Li-ion battery cell. As partially mentioned before, these are high energy 18650-type battery cells, with a capacity of $3350\,\mathrm{mAh}$, a maximum discharge current of $10\,\mathrm{A}$ and a voltage range from $2.5\,\mathrm{V}$ to $4.2\,\mathrm{V}$.

A. Measurement verification

The verification of the battery voltage measurement was done by measuring the voltage directly on the PCB, using an oscilloscope. While this was mainly done to verify the ESP32 measurements, any noise in the voltage is also visible.

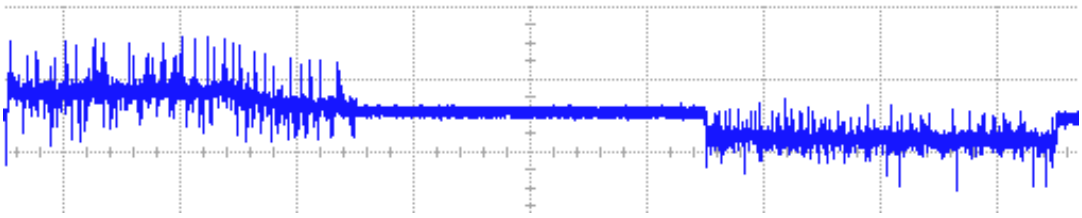

(a) Battery voltage response to the HPPC test, measured with a digital oscilloscope with 10 s per division horizontally and 200 mV per division vertically

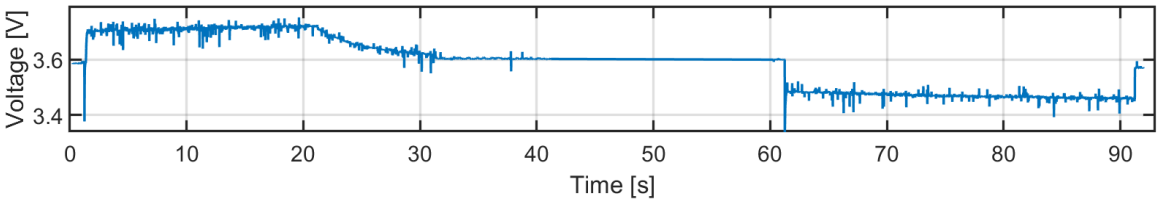

(b) Battery voltage response to the HPPC test, measured with the ESP32

Fig. 6: Comparison of the measurements performed by the ESP32 and by an oscilloscope

Specifically, two sets of voltage spikes are visible while current is flowing, shown in Figure 7 below. The initial oscillation has a maximum amplitude of $320\,\mathrm{mV_{P-P}}$, and the time between consecutive spikes is $6.4\,\mu\mathrm{s}$. This translates to a frequency of $156\,\mathrm{kHz}$, the switching frequency of the DCDC converter. There are also smaller spikes with an amplitude of $35\,\mathrm{mV_{P-P}}$, at the same frequency but with a time offset ($800\,\mathrm{ns}$ in the image). When the duty cycle of the DCDC converter changes, the time difference between the two voltage spikes changes but the amplitudes remain the same.

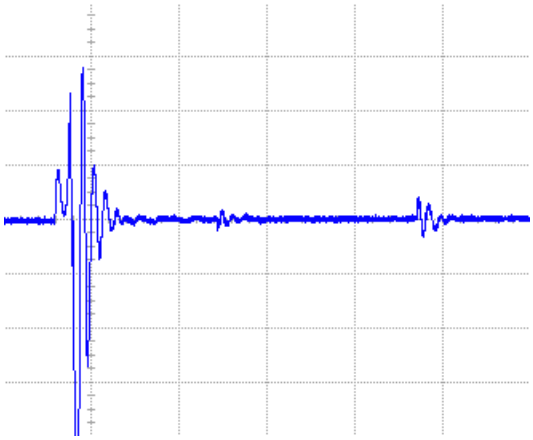

Fig. 7: Detailed voltage response while the HPPC test is active, measured with $200\,\mathrm{ns}$ per division horizontally and $50\,\mathrm{mV}$ per division vertically

When measuring the battery at the battery terminals, the large voltage spikes reduce to $100\,\mathrm{mV_{P-P}}$. This indicates that a large part of the spikes are generated by the gate drivers, specifically the bottom MOSFET which switches directly to ground.

The current from the battery was also measured and shows a similar noise spectrum to the voltage measurements, with the maximum noise $50\,\mathrm{mA_{P-P}}$ at a drive current of $500\,\mathrm{mA}$.

All this noise is high frequency, so partially filtered out by the capacitor placed at the inputs to the microcontroller, the result of which can be seen in Figure 6. This figure shows the two current pulses used in the HPPC test, measured by both the oscilloscope and the ESP32. The initial battery charging pulse has a drop in current and voltage starting at $20\,\mathrm{s}$ in Figure 6b, where the voltage of the supercapacitors drops too low which limits the current flow. This test is therefore unusable for the data processing, but it is used to verify the voltage measurements. As the shape of the measurements by both devices is the same, it confirms there is no drift in the voltage measurements of the ESP32.

The current also shows agreement between the oscilloscope and the ESP32. This means there is also no drift in the current measurement. However, the absolute current value is off by a factor 1.2, in both directions. The measured current is adjusted in the data processing step to its actual value, which is why the used data later shows $1.2\,\mathrm{A}$ instead of the intitial set current of $1\,\mathrm{A}$.

B. HPPC test results

The measured current and voltage, from a single charging pulse of the HPPC test, can be seen in respectively Figure 8 and Figure 9. These also show filtered data using a moving median, which filters out some of the high-frequency noise and speeds up the later data processing. A moving median is used as this does not affect the instantaneous voltage changes when the current starts and stops, which is important for the data processing.

The battery model is generated on both the charging and discharging pulse of the HPPC test. These two measurements give different values, as can be seen in Table I.

The difference in parameters is partially due to the battery having different internal parameters when charging or discharging, and partially due to errors in measurement and data fitting. An extreme case of the difference in charging and

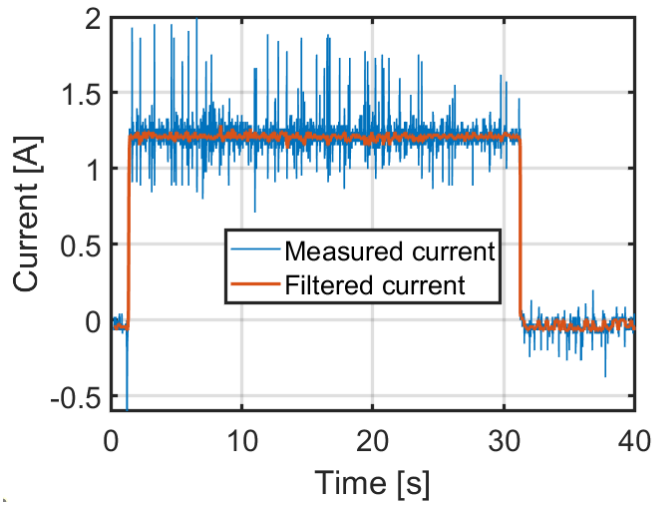

Fig. 8: Measured current during a charging pulse

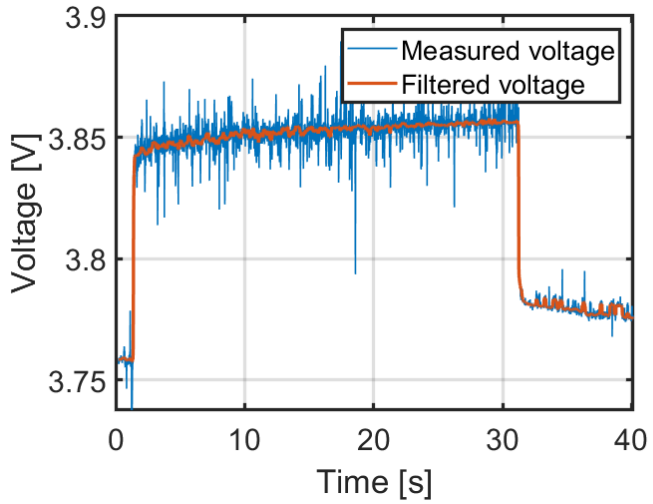

Fig. 9: Measured voltage during a charging pulse

discharging is seen at low battery SOC, depicted in Figure 10. The discharging pulse has a significantly larger voltage drop over time than the charging pulse. The last difference is due to the HPPC test itself, as the capacitors in the model are charged during the charging pulse and not entirely discharged when the second pulse occurs. In reality, this charge is due to the chemical processes not yet reaching equilibrium.

As the battery model used can only use a single value for each component, a combination of the charge and discharge

TABLE I: Battery model parameters

Parameter	Value HPPC charging	Value HPPC discharging
V_{OCV}	3.55V	3.55V
R_0	47.3mΩ	65.3mΩ
R_1	34.0mΩ	10.9mΩ
C_1	637mF	528mF
R_2	15.8mΩ	28.3mΩ
C_2	564F	641F

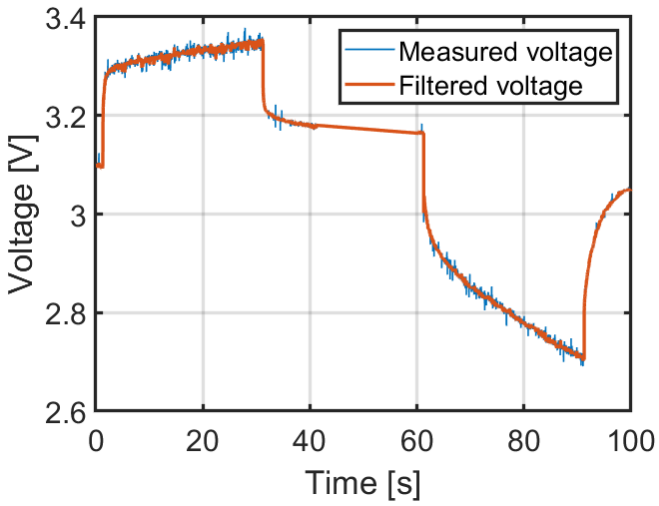

Fig. 10: Voltage response to a HPPC test at low battery SOC, showing both the charging and discharging pulse

variables is used in the final model. R_0, R_1 and C_1 are taken from the charging pulse, as there is no initial charge in the two capacitors of the model for this measurement, so the entire voltage response of the battery is due to the applied current. R_2 and C_2 are taken from the discharging pulse as there appears to be less noise present in those measurements, possibly due to the lower battery voltage while it is discharging. The parameters from the discharging pulse also fit better to the discharging battery data when the SOC of the battery is low, which is important for the SOP determination. This combination of parameters also showed the best results when doing the model verification, discussed later in Section IV-D.

C. EIS results

The results from the EIS test can be seen in the Nyquist plot of Figure 11.

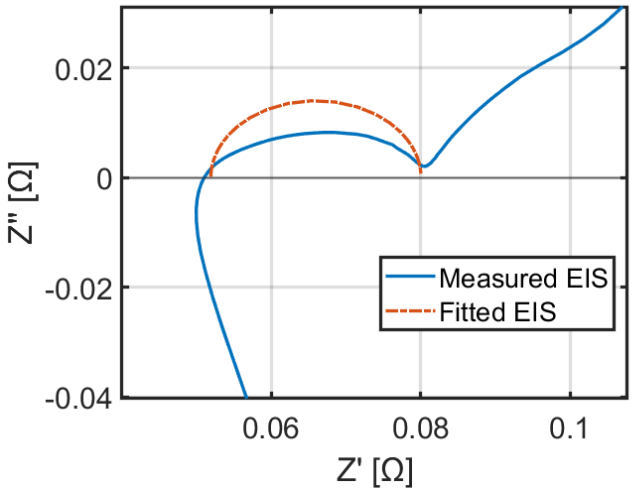

Fig. 11: Measured impedance from the EIS test, compared to the model generated through data fitting

This figure also shows the result gathered by fitting part of the battery model to this data. Specifically, the EIS data fitting is only done for R_0, R_1 and C_1 of the battery model. R_2 and C_2 would be fitted for $Z' > 0.08\,\Omega$. However, the fitting becomes uncertain and highly dependent on the selected data point on which the fitting is applied, which is why any comparison would also be uncertain for these two parameters.

From the partial battery model generated with the EIS test, the variables R_0, R_1 and C_1 of the HPPC test are still validated. The values gathered by each test, for the same battery, can be seen in Table II. V_{OCV} is not visible in the measured data of the EIS test, but it was gathered before the test started.

TABLE II: Battery model parameters for the HPPC and EIS tests

Parameter	Value HPPC	Value EIS
V_{OCV}	3.55V	3.52V
R_0	47.3mΩ	52.0mΩ
R_1	34.0mΩ	28.1mΩ
C_1	637mF	235mF
R_2	28.3mΩ	-
C_2	641F	-

It is clear from this data that most variables are close, but C_1 has a large difference. This difference will be partially due to the current rise in the HPPC test, as any non-instantaneous rise hinders the determination of the C_1 value from the HPPC test. It is also due to the $10\,\mathrm{ms}$ interval of the HPPC measurements. The RC time is only $0.0281 \cdot 0.235 = 6.6\,\mathrm{ms}$, so lower than this measurement interval.

The EIS test was also performed for other SOCs, which found similar issues.

D. Model verification

With only part of the battery model verified using the EIS measurements, the accuracy of the entire model is still unknown. The full verification is done with the current shown earlier in Figure 2. The measured voltage, as well as the simulated voltage with the generated battery model, can be seen in Figure 12.

As can be seen from the figure, The fast response from R_0, R_1 and C_1 shows a good correlation, but the slower voltage response due to R_2 and C_2 is too fast according to the model. The maximum voltage difference in this test is $48\,\mathrm{mV}$, which occurs at $1.7\,\mathrm{min}$ ($102\,\mathrm{s}$).

This maximum voltage difference can be reduced by manually adjusting the parameters of the model. The lowest maximum voltage difference found is $28\,\mathrm{mV}$, occurring at $8.1\,\mathrm{min}$. This is achieved by multiplying C_2 of the battery model by 2.0. However, to keep the data processing consistent throughout the entire SOC range of the model, none of the parameters are adjusted manually for the final battery model generated.

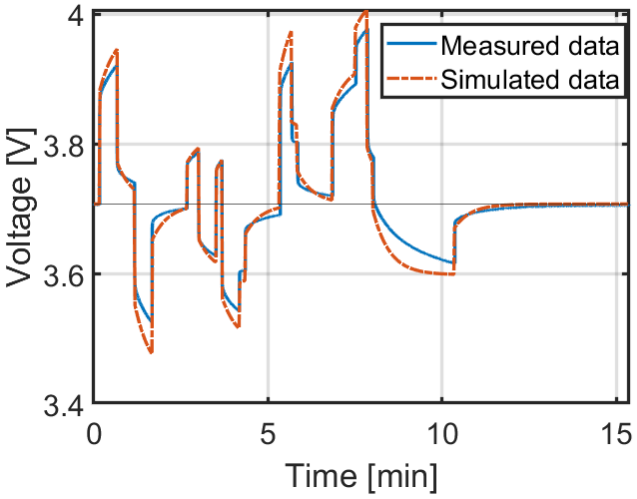

Fig. 12: Measured and simulated voltage according to the model

E. SOP model and result

As mentioned, the parameters of the battery model change according to the SOC. This also means the measurements have to be performed for different SOCs. This was done by measuring the battery in between charging cycles, where each charging cycle charged the battery for $250\,\mathrm{mAh}$. With the total capacitance of the battery being $3350\,\mathrm{mAh}$, this allowed for 14 different measurements. The battery was also relaxed for an hour after each charging cycle, before the HPPC test.

The resulting calculated resistances and capacitances of the battery model can be seen in Figure 13 and Figure 14. The battery is not measured when completely full or empty, as the battery voltage would exceed the manufacturer's voltage limits due to the high currents of the HPPC test.

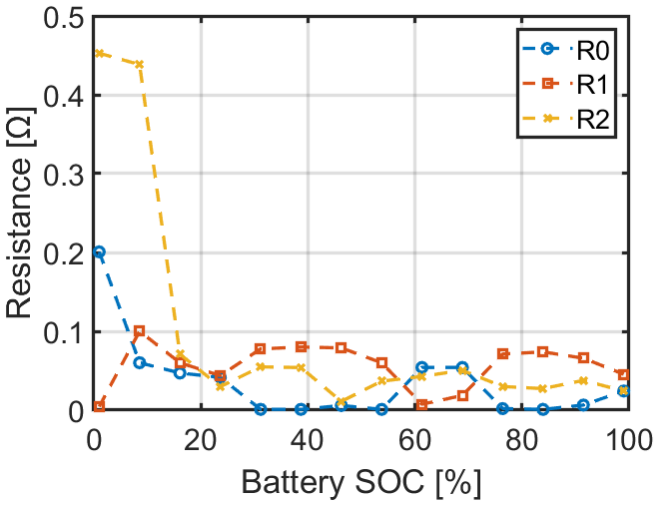

Fig. 13: Resistances of the battery model for different SOC

The change in parameters over the SOC is clearly visible in these figures, especially an increase in resistance when the battery is almost empty.

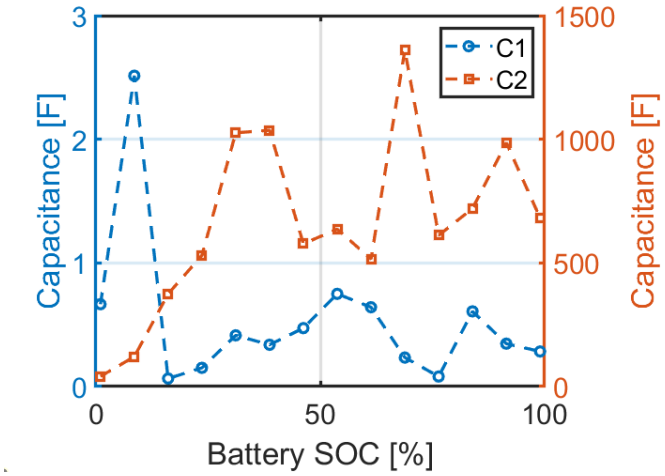

Fig. 14: Capacitances of the battery model for different SOC, with C_1 on the left axis and C_2 on the right axis

The full battery model can be used to determine the SOP of the battery through simulations. While this is dependent on the use case of the battery, two examples are given in Figure 15. The figure shows the power that can be drawn from the battery continuously, for both a 5 and a 30 minute duration, without exceeding the voltage or current limits of the battery. The current limit is $10\,\mathrm{A}$, the lower voltage limit is $2.5\,\mathrm{V}$. The x-axis depicts the initial charge of the battery.

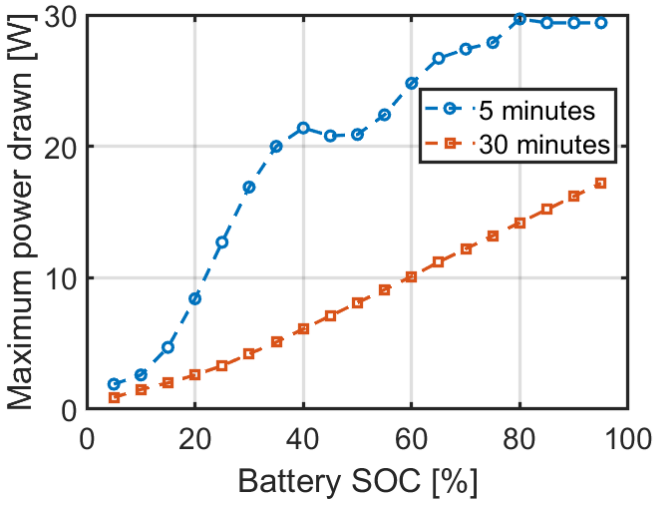

Fig. 15: Maximum power that can be drawn continually from the battery for a duration of 5 or 30 minutes, depending on the initial battery SOC

When withdrawing power for 30 minutes, the limiting factor is always the voltage when the battery is empty. When only using the battery for 5 minutes, the battery is limited by the current for high SOC and is limited by the voltage below a SOC of 35%. Even though the current is limiting, the maximum power is still changing for medium to high SOC. This is because the open circuit voltage of the battery drops as the SOC decreases, which in turn reduces the battery output power for the same current.

V. Discussion and Recommendations

It is clear from the results that the test setup is not perfect, both the measurements and the data processing can be improved. These are both shortly discussed, as well as any further steps that can be taken to develop the current prototype into a fully working system.

Specifically for the measurements, large voltage spikes are present in the battery voltage. While this is partially filtered out, the spikes will still have an impact on the data processing. The amplitude of the spikes can be reduced by lowering the switching speed of the MOSFETs, while the number of spikes can be lowered by slowing down the switching frequency. However, a slower switching frequency will increase the current ripple, which in turn can be reduced by using a larger inductor.

The current sensor used is a hall effect sensor, which was easy to implement but is not as precise as a shunt resistor measurement. Furthermore, the circuit design was made based on a maximum battery current of $10\,\mathrm{A}$. However, as mentioned, the current used for the HPPC test was only $1.2\,\mathrm{A}$. The lower current means the current sensor could have been chosen with a lower, but more precise, current range.

The data processing can also be improved. Currently, it uses a single MATLAB function, while a more specialised program can fit the model better to the data. By running the test multiple times, the model can also be improved through, for example, a Kalman filter [16].

Something that was not investigated is the battery model used. A second-order model is used, which does not represent all the chemical processes occurring inside the battery. This adds inaccuracies to the data processing. The model was chosen based on the literature found, but can be changed for future research.

The determined SOP was not verified, as it would be difficult to determine what part of any inaccuracies are due to generated model.

The prototype presented is only for a single battery cell. The final product should measure a battery pack, which requires several changes to the design. The most obvious changes are a higher required voltage and current for every part of the system. The required energy storage will therefore also be higher, so currently available supercapacitors do not seem relevant. Instead, a high-power battery can be used, the specifics of which have to be decided together with the DC-DC converter design. The simple converter design worked well, but can be improved through a tighter control loop. This can be done by separating the control and the measurements. The control loop only requires information about the current, while the data processing mainly uses the measured battery voltage. Only the current start time, end time and amplitude are required for the model generation.

VI. Conclusion

Using the portable battery measurement system presented in this paper, it is possible to create a battery model for a single li-ion cell. The second-order model used depicts instantaneous voltage changes due to electrical resistance in the battery, and also slower changes due to chemical processes.

The generated battery model shows the different parameters of the model over the entire SOC range, which allows the SOP to be determined if the initial charge of the battery is known.

However, the model generated is not perfect, due to both the measurements and the data processing. The measurements of battery voltage and current showed high-frequency noise, mostly as a result of the DC-DC converter build. The data processing is harder due to this noise, but negative effects on determining the battery model were mitigated by lengthening the HPPC test pulses. The data processing itself had some inaccuracies as well. Part of this is because of the simplicity of the data processing used, but it is also due to the specific battery model. Still, the generated model shows similarity to measured verification data, which proves the basic concepts work.

The main goals of the prototype, determining if a simple design works and the addition of the supercapacitors for energy storage, show promising results. The noise present due to the simplicity does have an impact, but mostly because more time is required to perform the test. The energy storage did limit the maximum current that can be used in the test, but this is easily fixed by increasing the total energy that can be stored. Otherwise, the energy storage only has an impact on the design of the DC-DC converter, and can be used to simplify this design as the specific voltage can be chosen.

In conclusion, even though the measurements were not ideal, the prototype designed and built shows good promise for the concept of the portable SOP tester, using its own energy storage instead of existing grid-dependent systems.

References

[1] A. Nagarajan. Western wind and solar integration study. [Online]. Available: https://www.nrel.gov/grid/wwsis.html

[2] N. K. Gupta, A. Kumar Singh, A. D. Thombre, and K. Pal, "Smart solar energy management to power computer lab in rural areas," in *2018 3rd International Innovative Applications of Computational Intelligence on Power, Energy and Controls with their Impact on Humanity (CIPECH)*, 2018, pp. 76–80.

[3] F. Amoroso, R. Hidalgo-León, J. Litardo, J. Urquizo, V. Villavicencio, M. Torres, P. Singh, and G. Soriano, "Simulation of an off-grid solar system to provide reliable energy access to the island community of bellavista in ecuador," in *2020 IEEE ANDESCON*, 2020, pp. 1–6.

[4] M. Kumar and B. Tyagi, "A small scale microgrid planning based on battery soc for a grid-connected microgrid comprising of pv system," in *2017 14th IEEE India Council International Conference (INDICON)*, 2017, pp. 1–5.

[5] International Energy Agency (IEA). Energy access outlook 2017. [Online]. Available: https://www.iea.org/reports/energy-access-outlook-2017

[6] S. Robic, Z. Morvaj, M. Olshanskaya, and R. Vrbensky, "Understanding energy poverty - case study: Tajikistan," in *21st World Energy Congress*, 2010.

[7] N. Chatrung, "Battery energy storage system (bess) and development of grid scale bess in egat," in *2019 IEEE PES GTD Grand International Conference and Exposition Asia (GTD Asia)*, 2019, pp. 589–593.

[8] X. Sun, N. Xu, Q. Chen, J. Yang, J. Zhu, J. Xu, and L. Zheng, "State of power capability prediction of lithium-ion battery from the perspective of electrochemical mechanisms considering temperature effect," *IEEE Transactions on Transportation Electrification*, pp. 1–1, 2022.

[9] C.-S. Huang, B. Balagopal, and M.-Y. Chow, "Estimating battery pack soc using a cell-to-pack gain updating algorithm," in *IECON 2018 - 44th Annual Conference of the IEEE Industrial Electronics Society*, 2018, pp. 1807–1812.

[10] A. Blidberg, "Correlation between different impedance measurement methods for battery cells," Master's thesis, KTH Royal Institute of Technology, Stockholm, Sweden, 2012.

[11] D. Deng, S.-Y. Liu, S.-L. Wang, L.-L. Xia, and L. Chen, "An improved second-order electrical equivalent modeling method for the online high power li-ion battery state of charge estimation," in *2021 IEEE 12th Energy Conversion Congress & Exposition - Asia (ECCE-Asia)*, 2021, pp. 1725–1729.

[12] A. Zenati, P. Desprez, and H. Razik, "Estimation of the soc and the soh of li-ion batteries, by combining impedance measurements with the fuzzy logic inference," in *IECON 2010 - 36th Annual Conference on IEEE Industrial Electronics Society*, 2010, pp. 1773–1778.

[13] S. Thanagasundram, R. Arunachala, K. Löffler, T. Teutsch, and A. Jossen, "A cell level model for battery simulation," in *European Electric Vehicle Congress Brussels*, 11 2012.

[14] Z. Li, X. Shi, M. Shi, C. Wei, F. Di, and H. Sun, "Investigation on the impact of the hppc profile on the battery ecm parameters' offline identification," in *2020 Asia Energy and Electrical Engineering Symposium (AEEES)*, 2020, pp. 753–757.

[15] X. Han, D. Guo, X. Feng, L. Lu, and M. Ouyang, "Equivalence of time and frequency domain modeling for lithium ion batteries," in *2021 IEEE 30th International Symposium on Industrial Electronics (ISIE)*, 2021, pp. 1–4.

[16] F. Khanum, E. Louback, F. Duperly, C. Jenkins, P. J. Kollmeyer, and A. Emadi, "A kalman filter based battery state of charge estimation matlab function," in *2021 IEEE Transportation Electrification Conference & Expo (ITEC)*, 2021, pp. 484–489.